HHS Public Access

Author manuscript

Heart Rhythm. Author manuscript; available in PMC 2024 May 01.

Published in final edited form as:

Heart Rhythm. 2023 May ; 20(5): 730–736. doi:10.1016/j.hrthm.2023.01.021.

miR-448 regulates potassium voltage-gated channel subfamily A member 4 (KCNA4) in ischemia and heart failure

Gyeoung-Jin Kang, PhD[1], **An Xie, PhD**[1], **Eunji Kim, PhD**[1], **Samuel C. Dudley Jr., MD, PhD**[1]

[1]Lillehei Heart Institute, University of Minnesota, Minneapolis, MN 55455

Abstract

Background—MicroRNA, miR-448, mediates some of the effects of ischemia on arrhythmic risk. Potassium Voltage-gated Channel Subfamily A Member 4 (*KCNA4*) encodes a $K_v1.4$ current that opens in response to membrane depolarization and is essential for regulating action potential duration in heart. KCNA4 has a miR-448 binding site.

Objective—Therefore, we investigated whether miR-448 was involved in the regulation of *KCNA4* mRNA expression in ischemia.

Methods—Quantitative real-time reverse-transcriptase polymerase chain reaction was used to investigate the expression of *KCNA4* and miR-448. Pull-down assays were used to examine the interaction between miR-448 and *KCNA4*. A miR-448 decoy and binding site mutation were used to examine specificity of the effect for *KCNA4*.

Results—The expression of *KCNA4* is diminished in ischemia and human HF tissues with ventricular tachycardia. Previously, we have shown miR-448 is upregulated in ischemia, and inhibition can prevent arrhythmic risk after myocardial infarction. The 3'-UTR of *KCNA4* has a conserved miR-448 binding site. MiR-448 bound to this site directly and reduced *KCNA4* expression and the transient outward potassium current (Ito). Inhibition of miR-448 restored *KCNA4*.

Conclusion—These findings showed a link between $K_v1.4$ downregulation and miR-448-mediated upregulation in ischemia, suggesting a new mechanism for the antiarrhythmic effect of miR-448 inhibition.

Keywords

Arrhythmias; Cardiology; Potassium channels; hypoxia; miRNA

Corresponding author: Samuel C. Dudley Jr., VCRC 286 - MMC 508, 425 Delaware St., SE, Minneapolis, MN 55455. sdudley@umn.edu.

Author contributions: GJK and SCD conceived and planned the experiments. GJK, AX, and EJK carried out the experiments. GJK took the lead in writing the manuscript. SCD supervised the work. All authors provided critical feedback and helped shape the research, analysis and manuscript.

Conflict of interest statement: The authors have no conflicts of interest to disclose.

Introduction

Cardiac ischemia is linked to an increased incidence of arrhythmia, although effective therapies are limited.[1, 2] Previous research has demonstrated that the control of various ion channels is dependent on the balance of multiple processes such as gene transcription, RNA processing, protein synthesis, and post-transcriptional regulation by microRNA (miRNA; miR) or RNA-binding proteins.[3–7]

Although the detailed molecular mechanism of ischemia-induced ion channel downregulation remains unknown, our recent research discovered that ischemia-induced miR-448 reduces the expression of *SCN5A* (encoding $Na_v1.5$), which is important for cardiac electrical conduction, and that anti-miR-448 therapy can reduce the incidence of arrhythmias.[3] In addition, various other ion channels are predicted targets of miR-448.

Voltage-gated K^+ channels control membrane potential in many cells and action potential duration in cardiomyocytes. The *KCNA4* gene is expressed in brain and heart and encodes the α-subunit required for the $K_v1.4$ channel. This protein encodes a slowly inactivating transient outward K^+ currents ($I_{to,s}$) during action potential repolarization.[8, 9] Expression of *KCNA4* has been confirmed at the cardiac transcript and protein levels in various mammalian hearts, including humans.[10–16]

Here, we show that miR-448 is involved in the regulation of *KCNA4* through a specific binding site present in the 3'-untranslated regions (UTR) region of *KCNA4* and that inhibition of miR-448 function in hypoxia can prevent the *KCNA4* reduction.

Materials and Methods

Cell culture

RL14 cells are a commercially available cell line of human fetal ventricular cardiomyocytes (CMs) derived from non-proliferative primary cultures of human fetal heart tissue (ATCC, Manassas, VA).[17–19] RL14 cells were grown in DMEM/F-12 nutrient mixture (GE Healthcare Life Sciences, Logan, UT) supplemented with 12.5% (v/v) fetal bovine serum (Gibco, Grand Island, NY) and penicillin-streptomycin (10,000 U/mL; Gibco). Because RL14 cells do not have spontaneous electrical activity or inducible action potentials, human induced pluripotent stem cells (hiPSC)-derived CMs (iCell® CMs) were obtained from Cellular Dynamics International (Madison, WI). iCell® CMs were seeded and maintained using iCell® Cardiomyocyte Plating Medium and Maintenance Medium (Cellular Dynamics International). For hypoxic conditions, the cells were cultured in an hypoxic incubation chamber (STEMCELL Technologies, Vancouver, BC) using pre-incubated culture media or were treated with hypoxic-mimetic chemicals, desferrioxamine (DFX) and cobalt chloride ($CoCl_2$) (Sigma, St. Louis, MO).

Cell transfection

Syn-hsa-miR-448 miScript miRNA mimic and negative controls were purchased from Qiagen (Valencia, CA). The cells were transfected using HiPerFect Transfection Reagent (Qiagen) following the recommendations of the manufacturer. Plasmid DNA was transfected

into cultured cells using FuGENE® 6 Transfection Reagent (Promega Corporation, Madison, WI) following the manufacturer's protocol.

Plasmid constructions

Gene fragments for *KCNA4* 3'-UTR with or without mutations at the miR-448 binding site were obtained from Integrated DNA Technologies, Inc. (IDT, Coralville, IA). They were cloned into pGL3-Promoter vectors downstream of the luciferase open reading frame to create pGL3-Promoter-Luciferase *KCNA4* 3'-UTR wild type (WT) or mutation (Mut) vectors. A gene fragment for miR-448 acted as a decoy. The decoy was obtained from IDT and was cloned into pcDNA3.1(+) luciferase vector downstream of the luciferase open reading frame to create a pcDNA3.1(+)-Luciferase-miR-448 decoy vector. The miR-448 decoy sequence was designed and confirmed using the "miRNAsong" web tool. All DNA constructs were confirmed by DNA sequencing. Luciferase mRNA level was detected by qPCR. The mRNA level of luciferase was normalized with the mRNA level of EGFP, which was co-transfected as a control.

RNA preparation and real-time reverse transcription polymerase chain reaction

Total RNA was prepared using RNeasy Plus Mini Kit (Qiagen) according to the manufacturer's instructions. Reverse transcription was performed with LunaScript® RT SuperMix Kit (NEB, Ipswich, MA). A reverse transcription quantitative real-time PCR was performed with PowerUp SYBR™ Green PCR Master Mix (ThermoFisher Scientific, Waltham, MA) using the 7500Fast Real-Time PCR system (ThermoFisher Scientific). The primer sequences used are in the Supplementary Material. $2^{-\Delta Ct}$ method was used to compare the expression between each group and the relative fold change was calculated by the $2^{-\Delta\Delta Ct}$ method, and the measurements were normalized with respect to the endogenous control (*GAPDH*).

Pull-down assay using biotinylated miRNA

RL14 cells were transfected with miR-448 or control RNA biotinylated at the 3'-end and incubated for 24 h. Cells were rinsed with cold phosphate buffered saline (PBS) and cross-linked by 365 nm UV light irradiation. Cells were collected using a scraper, and incubated on ice for 20 min before centrifugation at 12,000 × g for 15 min at 4 °C. The extract was incubated for 1 h at 4 °C with 10 μL Streptavidin-magnetic beads, and the Streptavidin/biotin-miRNA/mRNA complex was washed 5 times with a wash buffer. Biotin-miRNA/mRNA complexes were eluted for 5 min at 42 °C in 250 μL of elution buffer.

Western blot

Cells were washed twice with ice-cold PBS and disrupted in Cell Lysis Buffer (Cell Signaling Technology, Danvers, MA) with Protease and Phosphatase Inhibitor Cocktail (ThermoFisher Scientific) on ice for 30 min. Cell lysates were centrifuged at 14,000 rpm for 15 min at 4°C, and the resultant supernatants were subjected to Western blotting. The total protein concentration was quantified using the Pierce™ BCA Protein Assay Kit (ThermoFisher Scientific). Proteins were separated by electrophoresis on a 4–15% Mini-PROTEAN® TGX™ Precast Protein Gels (Bio-Rad, Hercules, CA), after which samples

were transferred on to a polyvinylidene difluoride (PVDF) membrane. The membrane was treated with 5% skim milk for 1 h and incubated with $K_v1.4$ antibody (1:1000 dilution; PA5–85937, ThermoFisher Scientific), and β-actin (1:5000 dilution; A5441, Sigma) overnight at 4°C. After TBST washing, the membrane was incubated with horseradish peroxidase (HRP)-conjugated secondary antibody (1:5000, Bio-Rad) for 90 min at room temperature. The proteins were visualized with Pierce™ ECL Western Blotting Substrate (ThermoFisher Scientific) using the ChemiDoc™ XRS+ System (Bio-Rad). The images were analyzed using ImageJ software to measure band density. Band density was normalized with β-actin from three independent experiments.

Electrophysiology

hiPSC-derived CMs were trypsinized (0.25% trypsin-EDTA, Invitrogen, ThermoFisher Scientific) for 10 min and plated in 35 mm culture dishes at a cell density of ~100 cells/dish on the day before the experiments. To measure action potentials (APs), the culture medium was replaced with Tyrode solution contained (in mmol/L) 140 NaCl, 5.4 KCl, 1 $MgCl_2$, 10 HEPES, 1.8 $CaCl_2$, 0.33 NaH_2PO_4 and 5.5 glucose (pH 7.4). Glass patch pipettes (World Precision Instrument, Sarasota, FL, USA) were pulled to a resistance of 2–5 MΩ. For AP measurements, the intracellular solution consisted of (in mmol/L) 120 potassium gluconate, 20 KCl, 5 NaCl, 0.02 EGTA, 0.05 $CaCl_2$, HEPES, and 5 MgATP (pH 7.2). APs were recorded using whole-cell current-clamp in an Axopatch-200B amplifier (Molecular Devices, Sunnyvale, CA, USA). Membrane potential recordings performed in the current-clamp configuration were low pass filtered at 10 kHz and digitized at 20 kHz using a gap-free acquisition mode.[20] Ito recording was carried out by a published method.[21] In brief, bath solution was composed of the following (mmol/L): NMDG 160, KCl 5.4, MgC12 2, D-Glucose10, TTX 0.01, E-4301 0.001, Nifedipine 0.01 and HEPES 10 (pH adjusted to 7.4 HCl). The pipette solution was composed of the following (mmol/L): K^+-Gluconate 150, EGTA 5, MgATP 5, and HEPES 10 (pH adjusted to 7.2 KOH). Series resistance in the whole-cell mode was in the range of 3 to 4 MΩ; 80% to 90% series resistance compensation was always used. Voltage-clamp currents were low-pass filtered at 1 kHz and digitized at 5 kHz. Currents were elicited by a series of 0.4-second test potentials at 10-mV increments from −40 to +60 mV from a holding potential of −50 mV at a frequency rate of 0.25 Hz. Current amplitudes were normalized to the cell capacitance and expressed as pA/pF.

Human samples

Deidentified control heart tissue was a gift of Prof. J.A. Wasserstrom of Northwestern University. All control heart tissue was derived from patients suffered brain death because of a cerebral vascular accident and had no concomitant cardiac conditions before the heart was harvested. Deidentified HF heart tissues were obtained from Lillehei Heart Institute tissue bank at the University of Minnesota. HF patients had a history of ischemic cardiomyopathy that was confirmed by histological specimens prepared concomitantly with acquisition of the specimen. In the control and HF groups, specimens were from the left ventricle. Arrhythmic status was determined by record review.

Statistics

Statistical significance between groups was performed using Student's t-tests (paired and unpaired) or a one-way analysis of variance (ANOVA) with multiple comparisons tests corrected using the Bonferroni method. For all analyses, a p-value of less than 0.05 was considered significant. All data were analyzed using Prism software (version 8.0, GraphPad Software, San Diego, CA). The data presented represent the mean + or ± standard deviation (SD) or standard error (SE) as indicated.

Results

KCNA4 was downregulated in heart failure

Heart failure (HF) is known to be associated with prolonged QT interval on the surface electrocardiogram and correlate with cellular action potential prolongation that can be explained in part by a reduction in K^+ currents.[22, 23] To determine *KCNA4* expression under pathological conditions, we investigated at *KCNA4* expression in normal human heart tissue and HF patient heart tissue. The *KCNA4* level was lower in HF compared to normal controls, and the channel was even lower in HF patients with a history of malignant ventricular arrhythmias (Figure 1). These results indicate that *KCNA4* may have a role in the development of HF-associated arrhythmias.

KCNA4 was involved in alterations in the action potential

In order to investigate the effect of *KCNA4* on the cardiac action potential (AP), *KCNA4* mRNA expression and AP were studied in hiPSC-derived CMs treated with *KCNA4* shRNA. *KCNA4* expression was reduced in hiPSC-derived CMs by shRNA treatment (Figure 2A). *KCNA4* shRNA increased APD30 (action potentials duration at 30% repolarization) in single hiPSC-derived CM (Figure 2B). AP amplitude and beating frequency showed no significant alterations. These findings indicate that $K_v1.4$ has a role in cardiac action potentials.

KCNA4 was a direct target of miR-448

KCNA4 was predicted to be a miR-448 target, and sequence analysis confirmed a complementary binding region for miR-448 within the 3'-UTR of *KCNA4* mRNA. This binding site has been found to be highly conserved in various species, including humans and mice (Figure 3A). The interaction between miR-448 and *KCNA4* was investigated using a pull-down assay for Argonaute RISC Catalytic Component 2 (AGO2), a major factor in RNA-induced silencing complex (RISC) and biotin-tagged miRNA mimic (Figure 3B and Supplemental Figure 1). When miR-448 mimic with biotin conjugation at the 3'-end was pulled down, *KCNA4* mRNA was identified. This binding was specific to miR-448. *KCNA4* mRNA was also identified in the AGO2 pull down assay (Figure 3C and Supplemental Figure 1). As a control, the expression of *KCND3*, which is also involved in Ito, was studied. There were no significant difference in the miR-448 pulled down samples compared with control (Figure 3C). There were also no significant changes in other K channels, *KCNH2*, *KCNQ1*, and *KCNJ2* in the miR-448 pulled down samples (Data not shown). In addition, the WT and Mut miR-448 binding sites of the *KCNA4* 3'-UTR were cloned. First, by

demonstrating that luciferase (LUC) expression was increased in a DNA clone including the *KCNA4* 3'-UTR, we demonstrated that this region might be significant for *KCNA4* mRNA regulation (Figure 4A). LUC expression was reduced by miR-448 mimics in WT cardiomyocytes, while the inhibitory effect of miR-448 mimics was reduced in miR-448 binding site mutants (Figure 4B). These findings indicate that *KCNA4 was a* direct target of miR-448.

KCNA4 expression and function were regulated by miR-448

Next, we investigated whether miR-448 affects the expression and function of $K_v1.4$ (encoded by *KCNA4*). miR-448 mimics decreased $K_v1.4$ protein expression in RL14 cells and hiPSC-derived CMs (Figure 5A and Supplemental Figure 2). miR-448 mimics reduced *KCNA4* mRNA expression but not *KCND3* mRNA (Figure 5B) in hiPSC-derived CM. The cardiac transient outward potassium current in hiPSC-derived CMs was measured to investigate the influence of miR-448 mimic on *KCNA4* function. The peak cardiac transient outward potassium current in transfected hiPSC-derived CMs treated with the miR-448 mimic was lower in comparison to a control transfection (Figure 5B). Similar to the effect by *KCNA4* shRNA, miR-448 mimic also led to APD prolongation in hiPSC-derived CMs (Supplemental Figure 3). 4-aminopyridine (4-AP)-sensitive Ito was also suppressed by the miR-448 mimic (Supplemental Figure 4). These findings suggested that miR-448 affects the $K_v1.4$ current level in addition to the *KCNA4* mRNA level.

KCNA4 was downregulated by hypoxia

We studied whether hypoxia was a driver for the reduction in *KCNA4*. When compared to normoxia (21% O_2, Nx), 6 h of hypoxia (2% O_2, Hx) reduced the mRNA and protein level of *KCNA4* expression (Figure 6A and B). A similar effect on Kv1.4 protein by hypoxia was seen in hiPSC-derived CMs (Supplemental Figure 5). Furthermore, hypoxia-mimetic compounds such as desferrioxamine (DFX) and cobalt chloride ($CoCl_2$) also diminished *KCNA4* expression (Figure 6C and D).

Blockade of miR-448 rescued *KCNA4* reduction in hypoxia

LUC as a marker for *KCNA4* expression was lowered by DFX. Mutation of the miR-448 binding site whereas the suppressed the effect of DFX on *KCNA4* (Figure 7A). Furthermore, decoy treatment for miR-448 rescued the reduction of *KCNA4* by DFX (Figure 7B). These findings indicate that miR-448 was the mediator of the hypoxia-induced *KCNA4* depletion.

Discussion

Arrhythmia is one of the primary causes of mortality in ischemic cardiomyopathy.[2, 24, 25] Arrhythmias are known to be generated by structural and electrical remodeling, and downregulation of ion channels by multiple pathways leads to ventricular electrical remodeling. These processes include transcriptional dysregulation, RNA processing, RNA stability, translation efficiency, and post-translational control as revealed in our previous reports.[3–7] Upregulation of ion channels lowered by the above processes can reduce the incidence of arrhythmias[3, 26] and may be an alternate strategy to blocking ion channels for treatment of arrhythmia.

We have shown previously that miR-448 mediates a *SCN5A* reduction after myocardial infarction and that antagonism of miR-448 is antiarrhythmic.[3] A reduction in *SCN5A* is expected to reduced Na^+ current, a shortening of the AP, and a slowing of cardiac conduction. These are arrhythmogenic effects sufficient to explain our findings with miR-448 antagonism. Nevertheless, miR-448 has other predicted ion channel targets that may contribute to ischemia induced arrhythmias and the antiarrhythmic effect of miR-448 antagonism and one predicted target of miR-448 is *KCNA4*. Here, we showed decreased levels of *KCNA4* correlated with arrhythmic risk in human samples. We further showed that *KCNA4* shRNA or miR-448 mimic led to APD prolongation in hiPSC-derived CMs (Figure 2 and Supplemental Figure 3). The regulatory targets of miR-448 using "miRWalk"[27], a miRNA binding site prediction tools, include *SCN5A* and *KCNA4*, as well as other ion channels. This suggests that miR-448 arrhythmic effect may involve multiple channels and potentially other proteins that influence ion channels.

We investigated the mechanism of a reduction in *KCNA4* in HF. We found increased *KCNA4* mRNA instability and discovered that miR-448, which is known to be elevated during ischemia, bound to *KCNA4* mRNA and reduced *KCNA4* mRNA, protein, and current. Previously, we have shown that HIF1α and NF-κB upregulate miR-448 levels in response to ischemia.[3] In hypoxia, the expression of *KCNA4* was reduced, and when the function of miR-448 was suppressed by a binding site mutation or decoy treatment, the *KCNA4* level was recovered. Together with our prior findings, these data indicate that miR-448 is involved in changes in potassium channels as well as sodium channels and that restoration of reduced levels of both channels may be involved in the previously demonstrated antiarrhythmic effect.

Unexpectedly, our results showed that treatment with a miR-448 mimic had a limited effect on *KCNA4* mRNA. Previously, we reported that the Hu antigen R (HuR, encoded by ELAVL1) may stabilize *SCN5A* and reduce the risk of arrhythmia in cardiomyopathy.[5] The analysis of the AU-rich elements (ARE) site, which includes the HuR binding site, reveals that the *KCNA4* 3'-UTR site has multiple ARE sites. Some ARE sites, in particular, are positioned near the miR-448 binding site. The limited impact of the miR-448 mimic may be explained by the fact that contact with HuR, an mRNA stabilizing factor, in the *KCNA4* mRNA 3'-UTR could interfere with the interaction between miR-448 and 3'-UTR.

We found that *KCNA4* levels were reduced with cardiomyopathy. Our findings are consistent with the prolonged action potential found in mice and humans after MI and in the presence of $K_v1.4$ autoantibodies.[28] Nevertheless, there is controversy about the relationship between *KCNA4* expression, cardiac disease, and arrhythmic risk. $K_v1.4$ is lower in the rat chronic heart failure induced by left coronary artery ligation.[11] On the other hand in other studies, $K_v1.4$ is enhanced in a rat acute myocardial infarction and diabetic rat ventricle.[29, 30] Another complication is that there is variable expression of $K_v1.4$ in different by regions of the ventricle, and between the atrium and ventricle, suggesting that the relationship of $K_v1.4$ may vary by cardiac chamber.[13, 31] Moreover, many ion channels are altered in cardiomyopathic states. Therefore, there is still uncertainty about the strength of the relationship of $K_v1.4$ to arrhythmic risk.

Conclusion

We found that *KCNA4* was reduced in human cardiomyopathy and that *KCNA4* levels inversely correlated with arrhythmic risk. This reduction in *KCNA4* prolonged the AP and reduced Ito. Furthermore, miR-448 could regulate *KCNA4* by binding to its 3' tail in response to hypoxia. Therefore, part of the antiarrhythmic effect of miR-448 antagonism after MI may represent improvements in *KCNA4* levels.

Supplementary Material

Refer to Web version on PubMed Central for supplementary material.

Funding:

HL104025 and HL106592 awarded by the National Institutes of Health.

References

1. Ghuran AV, Camm AJ. Ischaemic heart disease presenting as arrhythmias. Br Med Bull 2001;59:193–210. [PubMed: 11756211]
2. Glancy DL, Atluri P, Rodriguez JF, Subramaniam PN. Cardiac arrhythmias during myocardial infarction. Proc (Bayl Univ Med Cent). Vol 282015:192–193.
3. Kang GJ, Xie A, Liu H, Dudley SC. MIR448 antagomir reduces arrhythmic risk after myocardial infarction by upregulating the cardiac sodium channel. JCI Insight Dec 2020;5.
4. Zhou A, Shi G, Kang GJ, Xie A, Liu H, Jiang N, Liu M, Jeong EM, Dudley SC. RNA Binding Protein, HuR, Regulates SCN5A Expression Through Stabilizing MEF2C transcription factor mRNA. J Am Heart Assoc Apr 2018;7.
5. Zhou A, Xie A, Kim TY, Liu H, Shi G, Kang GJ, Jiang N, Liu M, Jeong EM, Choi BR, Dudley SC. HuR-mediated SCN5A messenger RNA stability reduces arrhythmic risk in heart failure. Heart Rhythm Jul 2018;15:1072–1080. [PubMed: 29454929]
6. Gao G, Dudley SC. RBM25/LUC7L3 function in cardiac sodium channel splicing regulation of human heart failure. Trends Cardiovasc Med Jan 2013;23:5–8. [PubMed: 22939879]
7. Shang LL, Pfahnl AE, Sanyal S, Jiao Z, Allen J, Banach K, Fahrenbach J, Weiss D, Taylor WR, Zafari AM, Dudley SC. Human heart failure is associated with abnormal C-terminal splicing variants in the cardiac sodium channel. Circ Res Nov 2007;101:1146–1154. [PubMed: 17901361]
8. Wymore RS, Negulescu D, Kinoshita K, Kalman K, Aiyar J, Gutman GA, Chandy KG. Characterization of the transcription unit of mouse Kv1.4, a voltage-gated potassium channel gene. J Biol Chem Jun 28 1996;271:15629–15634. [PubMed: 8663090]
9. Wymore RS, Korenberg JR, Kinoshita KD, Aiyar J, Coyne C, Chen XN, Hustad CM, Copeland NG, Gutman GA, Jenkins NA. Genomic organization, nucleotide sequence, biophysical properties, and localization of the voltage-gated K^+ channel gene KCNA4/Kv1.4 to mouse chromosome 2/human 11p14 and mapping of KCNC1/Kv3.1 to mouse 7/human 11p14.3-p15.2 and KCNA1/Kv1.1 to human 12p13. Genomics Mar 15 1994;20:191–202. [PubMed: 8020965]
10. Kabakov AY, Sengun E, Lu Y, Roder K, Bronk P, Baggett B, Turan NN, Moshal KS, Koren G. Three-Week-Old Rabbit Ventricular Cardiomyocytes as a Novel System to Study Cardiac Excitation and EC Coupling. Front Physiol 2021;12:672360. [PubMed: 34867432]
11. Hong J, Fu S, Gao L, Cai Y, Lazartigues E, Wang HJ. Voltage-gated potassium channel dysfunction in dorsal root ganglia contributes to the exaggerated exercise pressor reflex in rats with chronic heart failure. Am J Physiol Heart Circ Physiol Aug 1 2021;321:H461–h474. [PubMed: 34270374]
12. Kilfoil PJ, Chapalamadugu KC, Hu X, Zhang D, Raucci FJ Jr., Tur J, Brittian KR, Jones SP, Bhatnagar A, Tipparaju SM, Nystoriak MA. Metabolic regulation of Kv channels and cardiac repolarization by Kvβ2 subunits. J Mol Cell Cardiol Dec 2019;137:93–106. [PubMed: 31639389]

13. Wickenden AD, Jegla TJ, Kaprielian R, Backx PH. Regional contributions of Kv1.4, Kv4.2, and Kv4.3 to transient outward K^+ current in rat ventricle. Am J Physiol May 1999;276:H1599–1607. [PubMed: 10330244]

14. London B, Wang DW, Hill JA, Bennett PB. The transient outward current in mice lacking the potassium channel gene Kv1.4. J Physiol May 15 1998;509 (Pt 1):171–182. [PubMed: 9547391]

15. Dixon JE, Shi W, Wang HS, McDonald C, Yu H, Wymore RS, Cohen IS, McKinnon D. Role of the Kv4.3 K^+ channel in ventricular muscle. A molecular correlate for the transient outward current. Circ Res Oct 1996;79:659–668. [PubMed: 8831489]

16. Tamkun MM, Knoth KM, Walbridge JA, Kroemer H, Roden DM, Glover DM. Molecular cloning and characterization of two voltage-gated K^+ channel cDNAs from human ventricle. Faseb j Mar 1 1991;5:331–337. [PubMed: 2001794]

17. Mahrouf-Yorgov M, Augeul L, Da Silva CC, et al. Mesenchymal stem cells sense mitochondria released from damaged cells as danger signals to activate their rescue properties. Cell Death Differ Jul 2017;24:1224–1238. [PubMed: 28524859]

18. Orozco P, Montoya Y, Bustamante J. Development of endomyocardial fibrosis model using a cell patterning technique: In vitro interaction of cell coculture of 3T3 fibroblasts and RL-14 cardiomyocytes. PLoS One 2020;15:e0229158. [PubMed: 32092082]

19. Alammari AH, Shoieb SM, Maayah ZH, El-Kadi AOS. Fluconazole represses cytochrome P450 1B1 and its associated arachidonic acid metabolites in the heart and protects against angiotensin II-induced cardiac hypertrophy. J Pharm Sci Jul 2020;109:2321–2335. [PubMed: 32240690]

20. Xie A, Zhou A, Liu H, Shi G, Liu M, Boheler KR, Dudley SC. Mitochondrial Ca^{2+} flux modulates spontaneous electrical activity in ventricular cardiomyocytes. PLoS One 2018;13:e0200448. [PubMed: 30001390]

21. Ma J, Guo L, Fiene SJ, Anson BD, Thomson JA, Kamp TJ, Kolaja KL, Swanson BJ, January CT. High purity human-induced pluripotent stem cell-derived cardiomyocytes: electrophysiological properties of action potentials and ionic currents. Am J Physiol Heart Circ Physiol Nov 2011;301:H2006–2017. [PubMed: 21890694]

22. Cubeddu LX. Drug-induced inhibition and trafficking disruption of ion channels: pathogenesis of QT Abnormalities and Drug-induced Fatal Arrhythmias. Curr Cardiol Rev 2016;12:141–154. [PubMed: 26926294]

23. Veerman CC, Verkerk AO, Blom MT, Klemens CA, Langendijk PN, van Ginneken AC, Wilders R, Tan HL. Slow delayed rectifier potassium current blockade contributes importantly to drug-induced long QT syndrome. Circ Arrhythm Electrophysiol Oct 2013;6:1002–1009. [PubMed: 23995305]

24. Gräni C, Benz DC, Gupta S, Windecker S, Kwong RY. Sudden cardiac death in ischemic heart disease: from imaging arrhythmogenic substrate to guiding therapies. JACC Cardiovasc Imaging 10 2020;13:2223–2238. [PubMed: 31864982]

25. Jagu B, Charpentier F, Toumaniantz G. Identifying potential functional impact of mutations and polymorphisms: linking heart failure, increased risk of arrhythmias and sudden cardiac death. Front Physiol Sep 20 2013;4:254. [PubMed: 24065925]

26. Liu M, Liu H, Parthiban P, Kang GJ, Shi G, Feng F, Zhou A, Gu L, Karnopp C, Tolkacheva EG, Dudley SC. Inhibition of the unfolded protein response reduces arrhythmia risk after myocardial infarction. J Clin Invest 09 15 2021;131.

27. Sticht C, De La Torre C, Parveen A, Gretz N. miRWalk: An online resource for prediction of microRNA binding sites. PLoS One 2018;13:e0206239. [PubMed: 30335862]

28. Suzuki S, Satoh T, Yasuoka H, Hamaguchi Y, Tanaka K, Kawakami Y, Suzuki N, Kuwana M. Novel autoantibodies to a voltage-gated potassium channel Kv1.4 in a severe form of myasthenia gravis. J Neuroimmunol Dec 30 2005;170:141–149. [PubMed: 16182377]

29. Gao X, Yu S, Guan Y, Shen Y, Xu L. Nucleoporin 50 mediates KCNA4 transcription to regulate cardiac electrical activity. J Cell Sci 09 15 2021;134.

30. Nishiyama A, Ishii DN, Backx PH, Pulford BE, Birks BR, Tamkun MM. Altered K^+ channel gene expression in diabetic rat ventricle: isoform switching between Kv4.2 and Kv1.4. Am J Physiol Heart Circ Physiol Oct 2001;281:H1800–1807. [PubMed: 11557574]

31. Dixon JE, McKinnon D. Quantitative analysis of potassium channel mRNA expression in atrial and ventricular muscle of rats. Circ Res Aug 1994;75:252–260. [PubMed: 8033339]

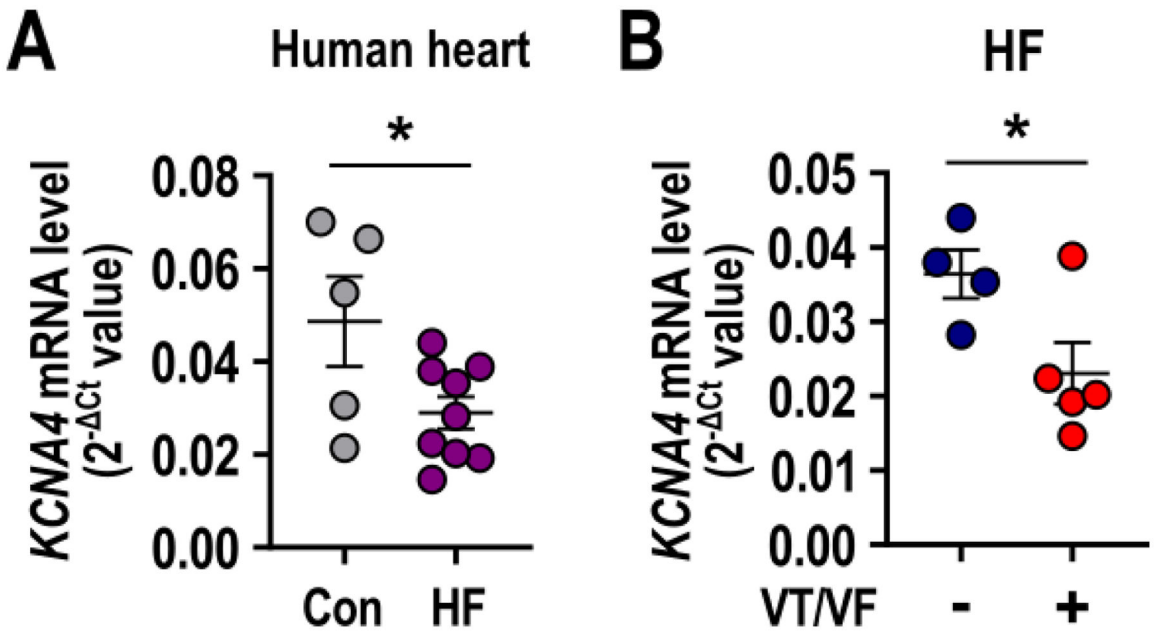

Figure 1.

KCNA4 decreases in human HF and correlated with arrhythmic risk. **A:** Expression of *KCNA4* in cardiac tissues from human control (Con) or HF patient. **B:** Expression of *KCNA4* in cardiac tissues from HF patient with or without ventricular tachycardia/ventricular fibrillation (VT/VF). Left ventricle tissue was obtained from control or heart failure patients (Healthy control n=5, HF n= 9). Data are represented as the mean ± standard error or mean (SEM). *, $P<0.05$ when compared between indicated groups by Student's t-test.

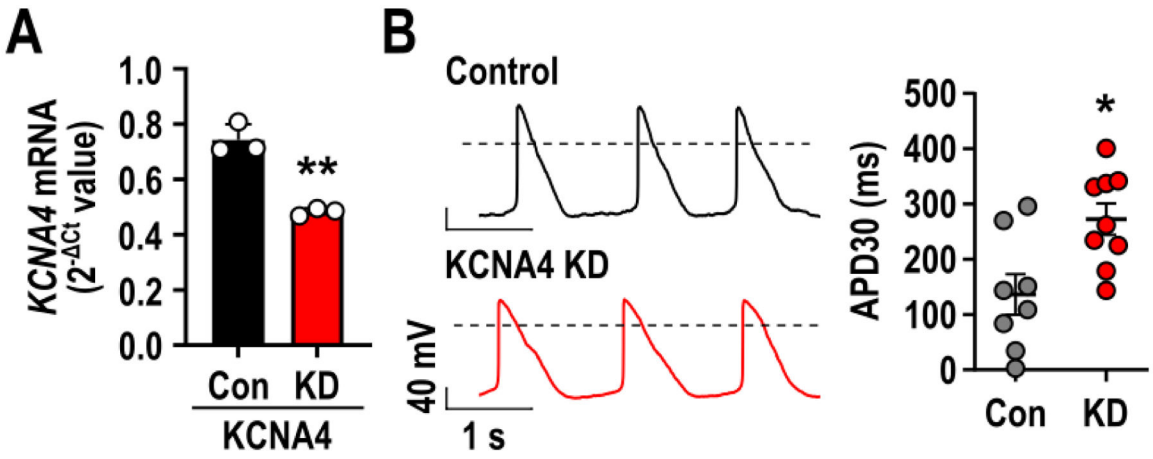

Figure 2.

KCNA4 is involved in the cardiac action potential duration. **A:** Effect of *KCNA4* shRNA on the expression of *KCNA4* in human iPSC-derived cardiomyocytes (CMs). **B:** Effect of *KCNA4* shRNA on the cardiac action potential in hiPSC-derived CMs. hiPSC-derived CMs were transfected with control or *KCNA4* shRNA and then incubated for 24 h. **C**: The effect of *KCNA4* shRNA on APD30.Data are shown as the mean + or ± SEM of three to four independent experiments. *, $P<0.05$; **, $P<0.01$ when compared between indicated groups by Student's t-test.

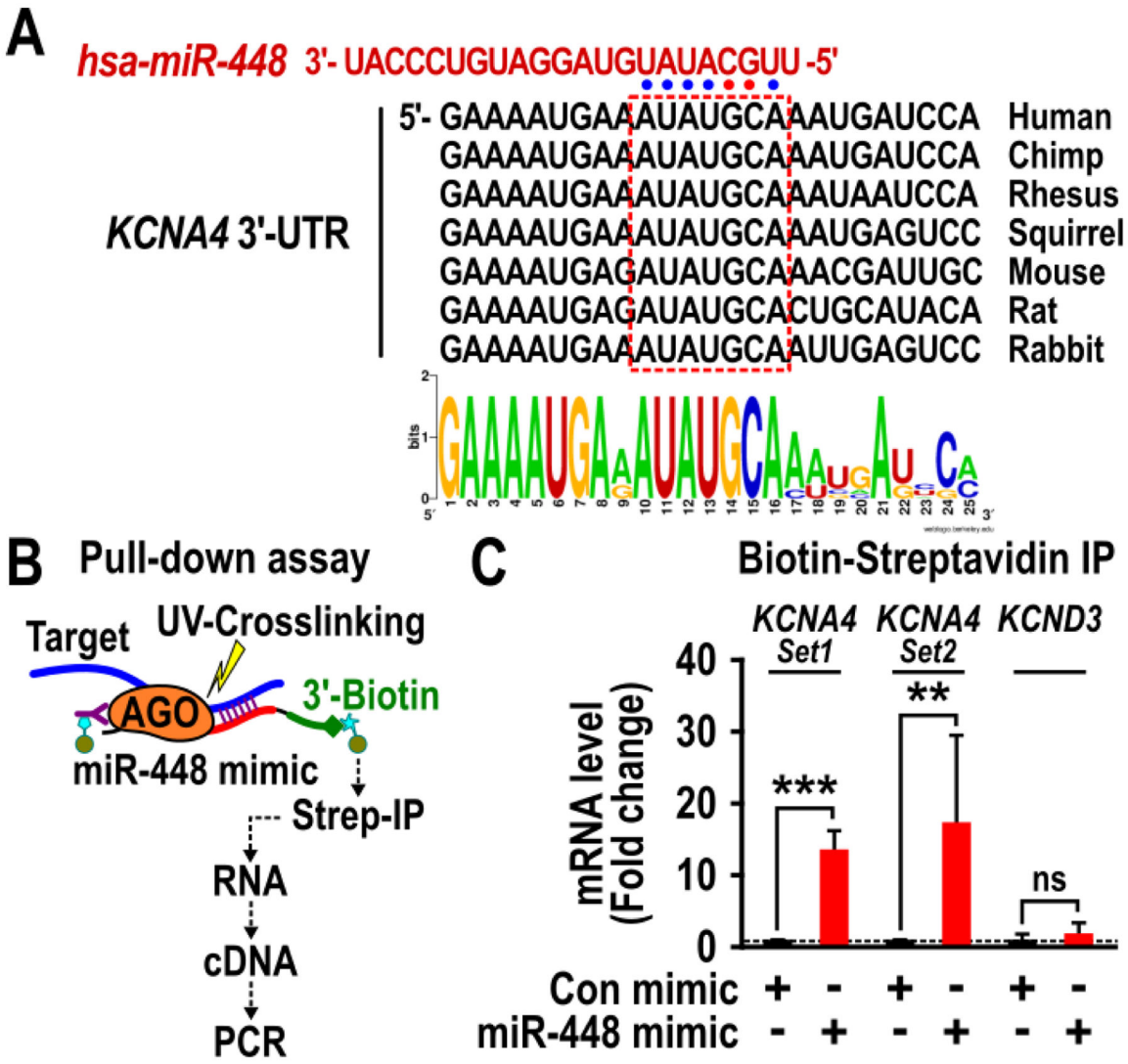

Figure 3.

The 3'-UTR of *KCNA4* contains a miR-448 binding site. **A:** Conserved miR-448 binding site of *KCNA4* 3'-UTR. **B:** Scheme of the pull-down assay. **C:** Pull-down analysis to confirm the binding between miR-448 and *KCNA4* mRNA in RL14 cells. 3'-End biotinylated control or miR-448 mimic were transfected into RL14 cells. Cells were cross-linked by irradiation with 365 nm UV light, and pulled down was done with Streptavidin-magnetic beads. Then, RNA was isolated and cDNA was synthesized to confirm the presence of *KCNA4* and *KCND3* mRNA by qPCR. Data are represented as the mean + SD of three to four independent experiments. **, $P<0.01$; ***, $P<0.001$ when compared between indicated groups by Student's t-test.

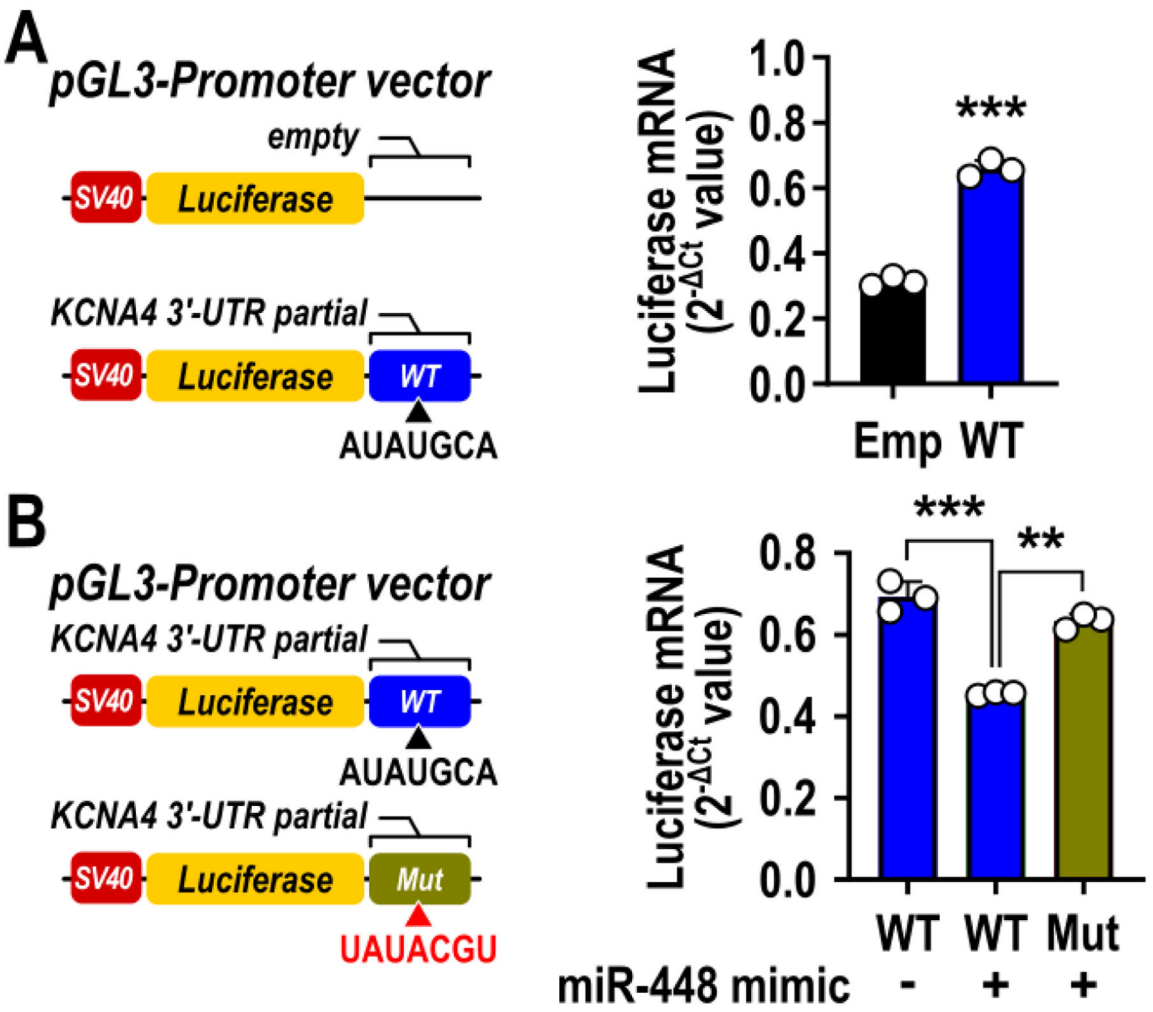

Figure 4.

KCNA4 mRNA is direct target of miR-448. **A:** Effect of *KCNA4* 3'-UTR on the luciferase (*LUC*) mRNA expression. **B:** Effect of miR-448 binding site mutation at *KCNA4* 3'-UTR on the *LUC* mRNA expression. WT or delMut for the miR-448 binding region in the *KCNA4* 3'-UTR were placed after the luciferase gene, respectively. RL14 cells were transfected with each DNA and then incubated for 24 h. As an expression control, EGFP DNA that was independently transfected was used. Data are represented as the mean + SD. **, $P<0.01$; ***, $P<0.001$ when compared between indicated groups by Student's t-test or 1-way ANOVA with Tukey multiple comparisons test.

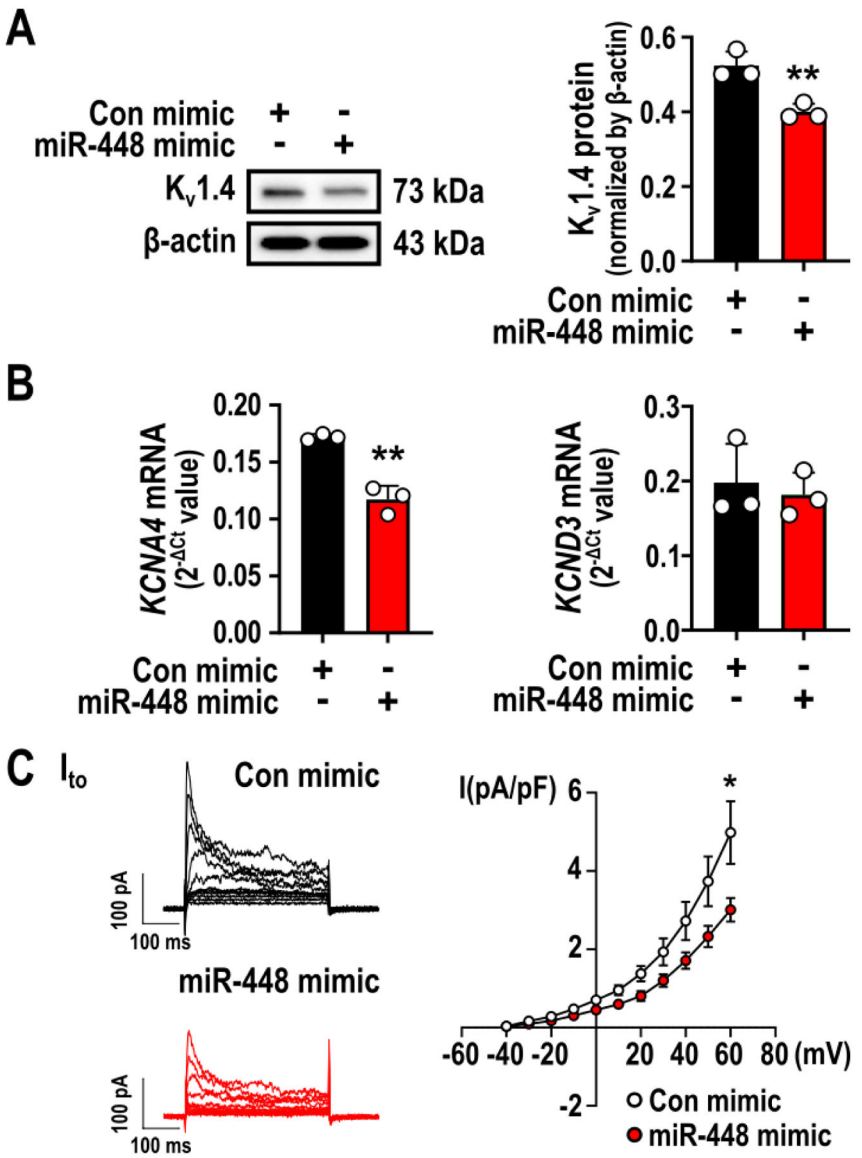

Figure 5.

miR-448 regulates *KCNA4* expression and function. **A:** Effect of miR-448 mimic on the protein expression of *KCNA4* ($K_v1.4$) in RL14 cells. **B:** Effect of miR-448 mimic on the mRNA expression of *KCNA4* and *KCND3* in hiPSC-derived CMs. **C:** Effect of miR-448 mimic on the transient outward potassium current (I_{to}) in hiPSC-derived CMs. Cells were transfected with control or miR-448 mimic and then incubated for 24 h. The expression of $K_v1.4$ and β-actin level were detected by Western blot. Data are represented as the mean + SD or ± SE of three to four independent experiments. *, $P<0.05$; **, $P<0.01$ when compared between indicated groups by Student's t-test.

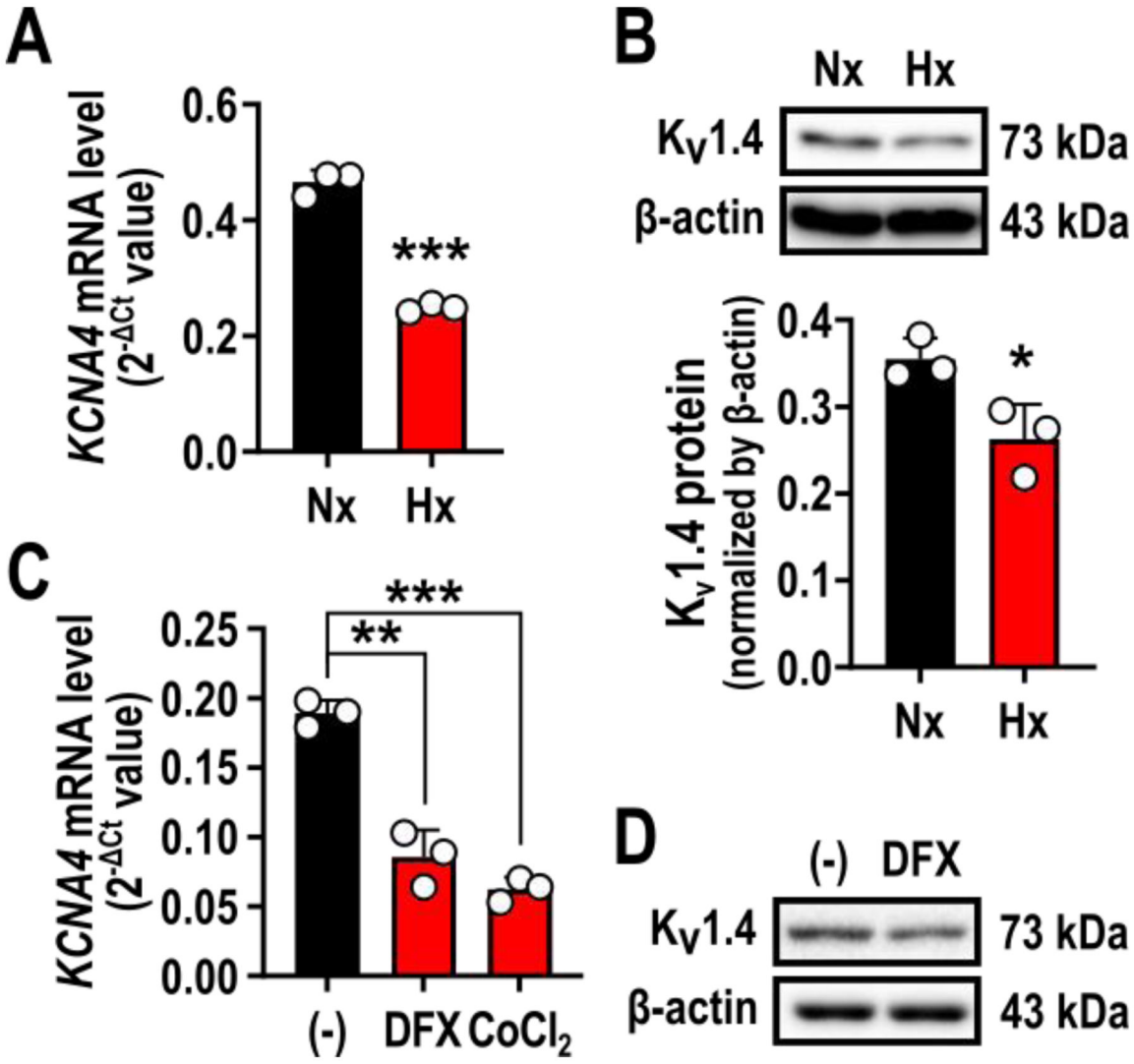

Figure 6.

KCNA4 is decreases in hypoxia. **A-B:** Effect of hypoxia on the mRNA and protein expression of *KCNA4*. **C-D:** Effect of hypoxia-mimetic condition on the mRNA or protein expression of *KCNA4*. hiPSC-derived CMs (panel A) or RL14 cells (panel B) were incubated in normoxic (21% O_2) and hypoxic (2% O_2) conditions for 6 h. RL14 cells were stimulated with desferrioxamine (DFX) and cobalt chloride ($CoCl_2$) for 24 h. Data are represented as the mean + SD of three independent experiments. *, $P<0.05$; **, $P<0.01$; ***, $P<0.001$ when compared between indicated groups by Student's t-test or 1-way ANOVA with Tukey multiple comparisons test.

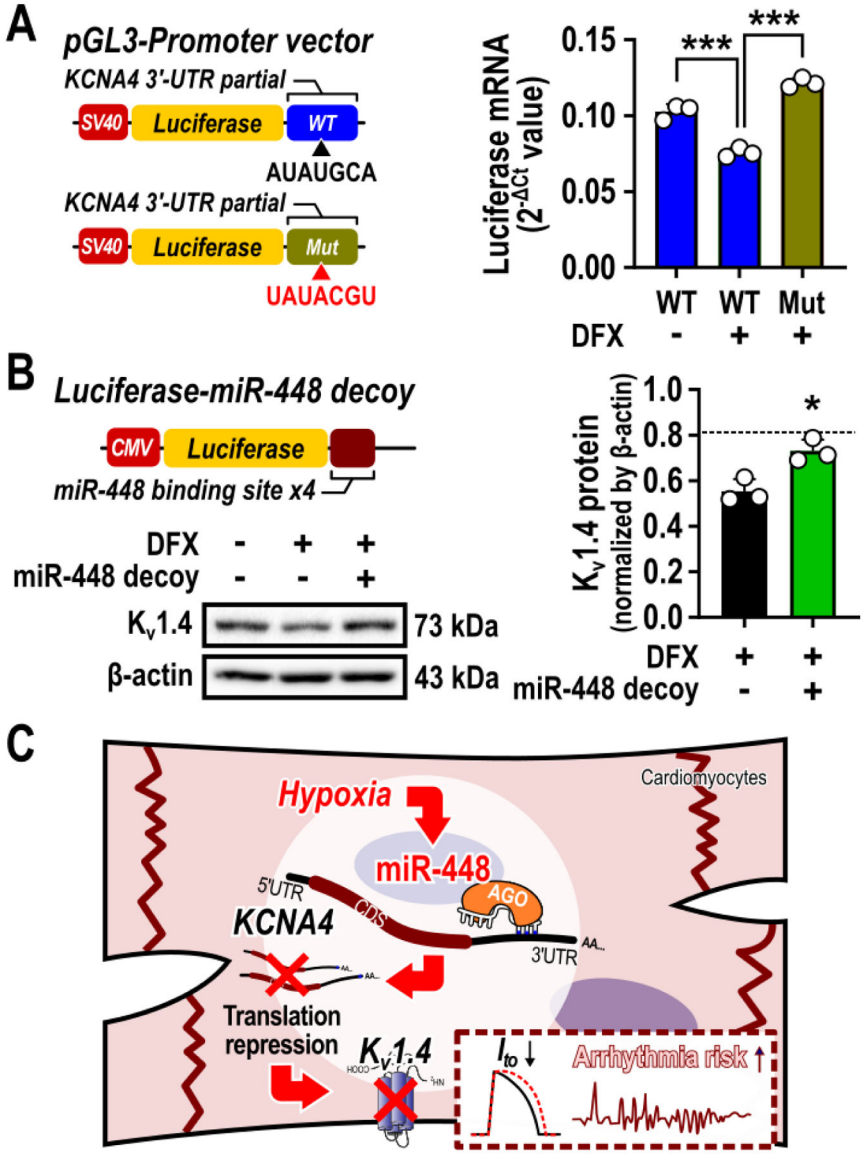

Figure 7.

Blocking of miR-448 function restores reduced *KCNA4* expression under hypoxic conditions. **A:** Effect of miR-448 binding site mutation at *KCNA4* 3'-UTR on the *LUC* mRNA expression in hypoxic condition. **B:** Effect of miR-448 decoy on the protein expression of *KCNA4*. **C:** Summary of the effect of miR-448 on *KCNA4* in hypoxia. RL14 cells were transfected with WT or delMut DNA for the miR-448 binding region of *KCNA4* 3'-UTR and then incubated for 24 h. As an expression control, EGFP DNA that was independently transfected was used. RL14 cells were transfected with miR-448 decoy and then were stimulated with DFX for 6 h. The expression of $K_v1.4$ and β-actin level were detected by Western blot. Dot line means normal $K_v1.4$ protein level. Data are represented as the mean + SD of three independent experiments. *, $P<0.05$; ***, $P<0.001$ when compared between indicated groups by Student's t-test.